Supplementary material

Predator and scavenger movements among and within endangered seabird colonies: opportunities for pathogen spread

Amandine Gamble, Romain Bazire, Karine Delord, Christophe Barbraud, Audrey Jaeger, Hubert Gantelet, Eric Thibault, Camille Lebarbenchon, Erwan Lagadec, Pablo Tortosa, Henri Weimerskirch, Jean-Baptiste Thiebot, Romain Garnier, Jérémy Tornos, and Thierry Boulinier

Appendix S1. Supplementary text and figures

Appendix S1.A. Study system

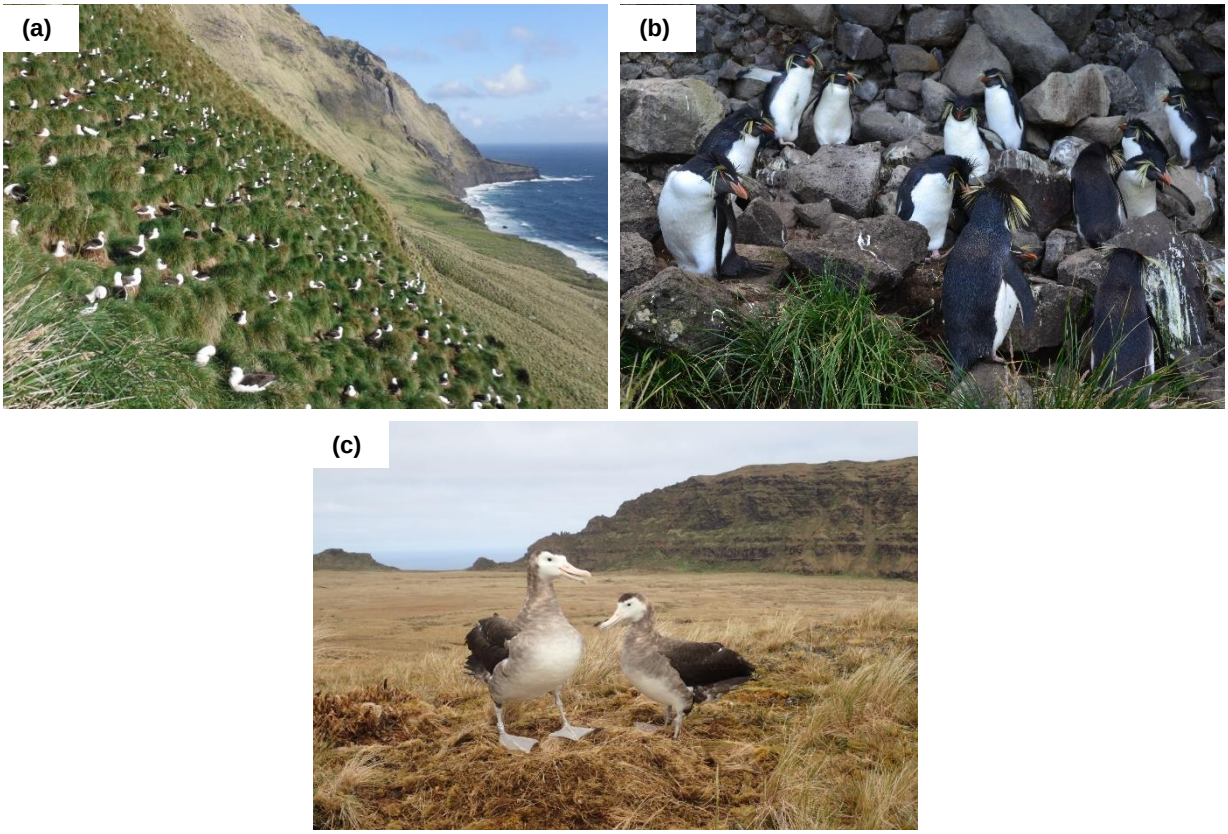

Figure S1.A.1. Seabirds of Amsterdam Island (37°49'S, 77°33'E). **a)** A colony of Indian yellow-nosed albatrosses (*Thalassarche carteri*) in Entrecasteaux (photo: Thierry Boulinier, IPEV). **b)** A colony of northern rockhopper penguins (*Eudyptes moseleyi*) in Entrecasteaux (photo: Nicolas Giraud, IPEV). **c)** A pair of Amsterdam albatrosses (*Diomedea amsterdamensis*) breeding on Plateau des Tourbières (photo: Nicolas Giraud, IPEV). Note that yellow-nosed albatrosses and rockhopper penguins gather in dense mono-specific colonies, contrasting with the low density of the unique Amsterdam albatross colony. Similarly to Amsterdam albatrosses, brown skuas (*Stercorarius antarcticus*) nest at low density. All those species but the skua forage exclusively at sea (Heerah *et al.* 2019).

Figure S1.A.2. Illustration of predator- and scavenger-prey interactions on Amsterdam Island. **a)** A brown skua eating the carcass of a yellow-nosed albatross nestling in Entrecasteaux cliffs during an avian cholera outbreak (photo: Marine Bely, IPEV). **b)** A brown skua eating a brown rat (*Rattus norvegicus*) at the Martin-de-Viviès station close to the Mare aux Éléphants skua club (photo: Adrien Coatanea, IPEV). **c)** A rodent biting a live yellow-nosed albatross nestling in Entrecasteaux cliffs during an avian cholera outbreak (photo: Marine Bely, IPEV). **d)** A brown rat scavenging on the carcass of a yellow-nosed albatross nestling in Entrecasteaux cliffs during an avian cholera outbreak (photo: Marine Bely, IPEV).

Appendix S2.B. Epidemiological data: supplementary methods and results

Immunoassays

This study is the first to report the detection of anti-*Pasteurella multocida* antibodies in skuas. In order to strengthen the inference of individual past exposure from the collected plasma samples, we combined two serological tests assessing different components of the humoral response. First, immunoglobulins Y (IgY) against whole *Pm* cells of serotypes Heddleston 1, 3, and 4 were detected using a commercial indirect enzyme-linked immunosorbent assay (ELISA; ID Screen® *Pasteurella multocida* Chicken and Turkey Indirect, IDvet, France). The use of anti-chicken IgY to detect seabird IgY has previously been validated (Garnier *et al.* 2017). Second, specific agglutinating antibodies (including notably IgM and IgY) were measured with a microagglutination test (MAT) developed using the serotype Heddleston 1 *Pm* strain isolated on Amsterdam Island during an albatross die-off (SEROPAST®, Ceva-Biovac, France; see Bourret *et al.* 2018). These methods are classically used in (veterinary) medicine, epidemiology and ecology to detect specific antibodies and thus past exposure to a given infectious agent (e.g., Tizard, 2004, Garnier & Graham, 2014).

The ELISA (ID Screen® *Pasteurella multocida* Chicken and Turkey Indirect, IDvet, France) was run following the manufacturer instructions. Raw optical density (OD) was read at 450nm and corrected for inter-plate variations following Lobato *et al.* 2011. Briefly, a set of six to height samples selected to represent a range of raw OD values were replicated across plates. For each plate combination, we then calculated the coefficients *a* and *b* of the linear regression of the raw OD values of these replicated samples on the two considered plates (all $r^2 \geq 0.97$, n = 6 to 8 samples on 11 plate pairs regrouping samples from the present study and those presented in Gamble *et al*. 2019). Corrected OD values were then calculated based on the raw OD values of the samples replicated across the different plates and using the following equation: corrected OD = $a \times$ (original OD) + b. Results are expressed as the corrected OD values, thereafter referred as OD values.

The seropositivity threshold was determined by fitting a mixture of normal distributions to the values of ODs (following Garnier *et al.* 2017) and assuming that OD values can be used to distinguish a group of seropositive and a group of seronegative individuals. The threshold value was estimated as the mean of the normal distribution followed by the negative samples + 3 standard deviations, corresponding to a 99% confident interval around the distribution of negative samples. This high value limits the risk of false positive. The microagglutination test (MAT; SEROPAST®, Ceva Biovac, France) was run following the procedure described in Bourret *et al.* 2018. Agglutination at 1:40 dilution was used as the seropositivity threshold as this was the highest titer recorded in the samples from a site where avian cholera is not known to circulate (n = 25; Falkland/Malvinas Islands; see below). Similarly, this high value limits the risk of false positive. Results are expressed as titre (log2[dilution/10]+1).

Evaluation and comparison of the immunoassays

Plasma samples from 25 brown skuas collected on another site than Amsterdam Island (Falkland/Malvinas Islands; 51°45'S, 59°00'W; samples provided by Jacob González-Solís, Universitat de Barcelona, Spain) were also analysed and their antibody levels used to improve the calculation of the ELISA positivity threshold and to compare the two immunoassays. All samples except two were analysed by MAT and ELISA. Both immunoassays proved successful to quantify anti-*P. multocida* antibodies in yellow-nosed albatrosses on Amsterdam Island using an

experimental approach based on a vaccination design using the locally circulating strain (Bourret *et al.* 2018).

Agreement between qualitative outcomes (i.e., negative or positive) of the two immunoassays was assessed by Cohen's kappa coefficient using the '*psych*' R package (Revelle 2014). For the ELISA-positive samples, the correlation between the quantitative outcomes of the two immunoassays was assessed by a major axis regression using the '*lmodel2*' R package (Legendre 2013). For kappa coefficient, $\kappa \leq 0.4$ indicates a poor agreement, $0.4 < \kappa \leq 0.8$ indicates a fair to good agreement, and $\kappa > 0.8$ indicates an excellent agreement (Fleiss 1981). Because the two immunoassays were designed to target different immunoglobulins binding different antigens, the agreement between their outcomes was expected to be good but not perfect. Results are indicated with 95% confidence interval indicated between brackets.

The MAT proved to be repeatable ($r^2 = 0.87$, n = 10 samples). Regarding the ELISA, high repeatability was observed both at intra-plate ($r^2 = 0.98$, n = 10 samples) and inter-plate (all $r^2 \geq 0.97$, n = 6 to 8 samples on 11 plate pairs) levels. The ELISA positivity threshold was estimated at 0.04 (Figure S1.B.1). Agreement between the qualitative results of the two assays (MAT and ELISA) was almost perfect ($\kappa = 0.96$ [0.89; 1.00], $p < 0.01$, n = 98; one sample was MAT-positive and ELISA-negative, and one reciprocally). Quantitative results were also positively correlated ($\beta = 0.13$ [0.07; 0.19], $p = 0.01$, $r^2 = 0.24$, n = 63; Figure S1.B.2). Note also that the seronegativity of some individuals is an interesting observation as it shows an absence of cross-reactivity of the immunoassays to skuas' plasmatic proteins.

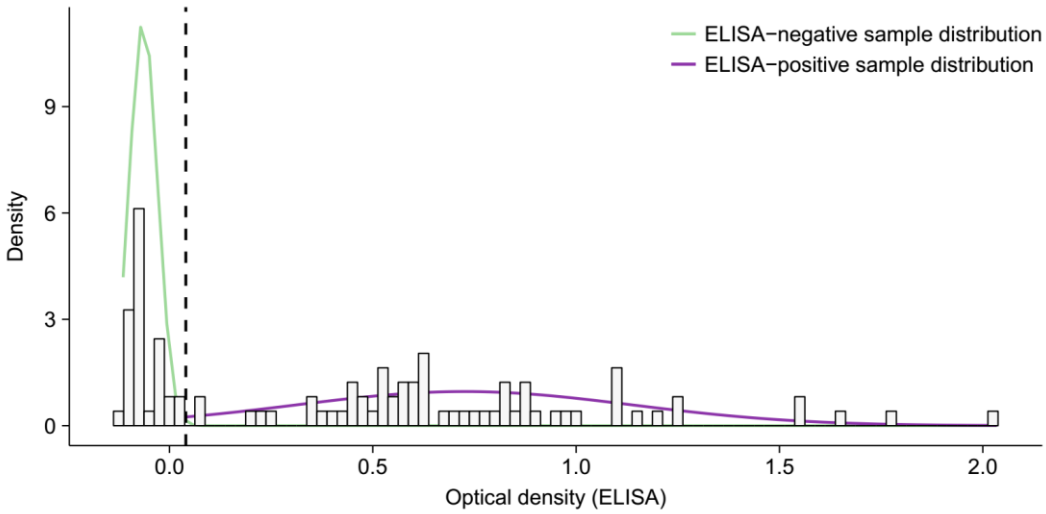

Figure S1.B.1. Distribution of optical densities for brown skuas used to quantify the immune response against *P. multocida* by ELISA. The histograms present the normalized counts of individuals and the curves correspond to the probability density function of the two corresponding normal distributions (negative and positive samples). The threshold value (dashed line) was estimated as the mean of negative normal + 3 standard deviations. This graphic represents 72 samples from Amsterdam Island and 25 from another site (Falkland/Malvinas Islands; samples provided by Jacob González-Solís).

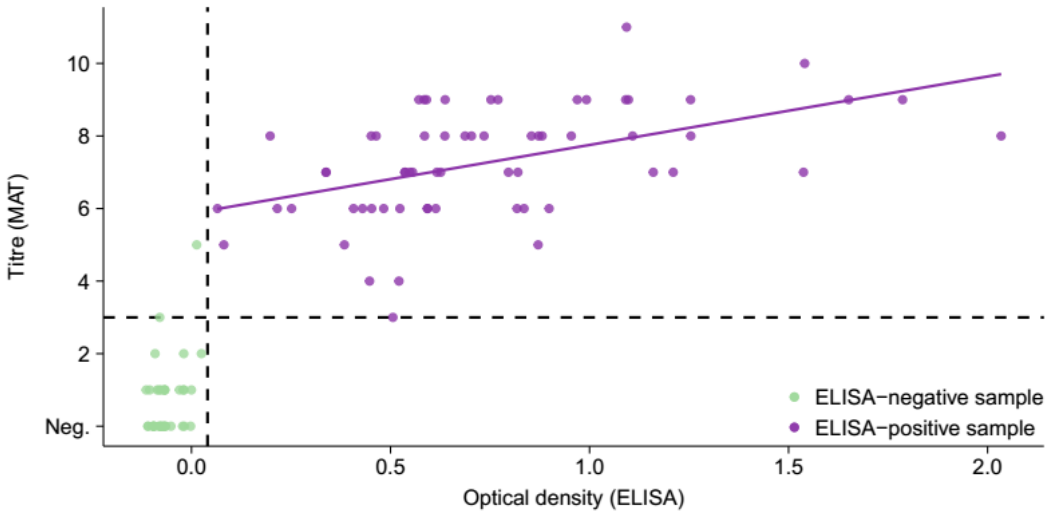

Figure S1.B.2. Correlation between *P. multocida* specific antibody levels in brown skua using the ELISA and MAT. Seropositivity threshold values are represented by the dashed lines (vertical for the ELISA and horizontal for the MAT). The solid line represents the regression conducted on ELISA-positive samples. This graphic represents 72 samples from Amsterdam Island and 25 from another site (Falkland/Malvinas Islands; samples provided by Jacob González-Solís).

Molecular detection by real-time polymerase chain reaction

Detection of *P. multocida* DNA in cloacal swab samples was performed using the real-time polymerase chain reaction (RT-PCR) protocol described in Jaeger et al. 2019 and designed using the sequence of the D2C *P. multocida* strain isolated from a sooty albatross found dead on Amsterdam Island in 2011 (Jaeger et al., 2018). Concretely, we used the *P. multocida* for (5'-ACGGCGCAACTGATTGGACG-3') and *P. multocida* rev (5'-GGCCATAAGAAACGTAACTCAACA-3') primers allowing the amplification of a 116 nucleotides amplicon within KMT1 gene, a locus routinely used for the detection of *P. multocida* through end-point PCR (Townsend, Frost, Lee, Papadimitriou, & Dawkins, 1998). Amplification was monitored in a Stratagene MX3005P (Agilent Technologies, Santa Clara, USA) thermocycler using the fluorescent *P. multocida* probe (5'FAM-TCAGCTTATTGTTATTTGCCGGT3'BHQ1). Amplifications were performed in 25 µL final volume containing 12.5 µL of Absolute Blue real-time PCR Low Rox Mix (Thermo Scientific, Waltham, MA, USA), 0.4 µM of each primer and 0.2 µM of Pm-probe. The PCR conditions included a first Taq-Polymerase activation step (95°C for 15 min), followed by 40 cycles each composed of a denaturation (95°C for 15 sec.), an annealing (54°C for 30 sec.) and an extension (72°C for 30 sec.) step.

Comparison of antibody levels among sites and years

Table S1.B.1. Comparison of antibody levels among capture sites and years. Antibody levels were expressed as ODs resulting from ELISA. Statistical significance of observed differences in antibody levels among locations within a year or among years in a location were investigated using Wilcoxon tests with a Bonferroni correction for multiple testing (set of eight tests) and a 5% significant level. Statistically significant differences are highlighted in the table by bold p-values. The corresponding data are presented in Figure 3a. PDT: Plateau des Tourbières; MAE: Mare aux Éléphants.

	Sample 1 Site, year (sample size)	**Sample 2** Site, year (sample size)	**Wilcoxon statistics**	**Corrected p-value**
Site comparison	PDT, 2015-2016 (10)	Entrecasteaux, 2015-2016 (10)	17	0.0920
	PDT, 2016-2017 (10)	MAE, 2016-2017 (10)	4	**0.0044**
	PDT, 2016-2017 (10)	Entrecasteaux, 2016-2017 (10)	43	1.0000
	MAE, 2016-2017 (10)	Entrecasteaux, 2016-2017 (10)	80	**0.0004**
Year comparison	PDT, 2011-2012 (16)	PDT, 2015-2016 (10)	41	0.3268
	PDT, 2011-2012 (16)	PDT, 2016-2017 (10)	46	0.6177
	PDT, 2015-2016 (10)	PDT, 2016-2017 (10)	50	1.0000
	Entrecasteaux, 2015-2016 (10)	Entrecasteaux, 2016-2017 (10)	28	0.8410

Exploration of the potential effect of sex on birds' epidemiological status

Tarsus and skull lengths were measured on each bird captures in 2015-2016 and 2016-2017.

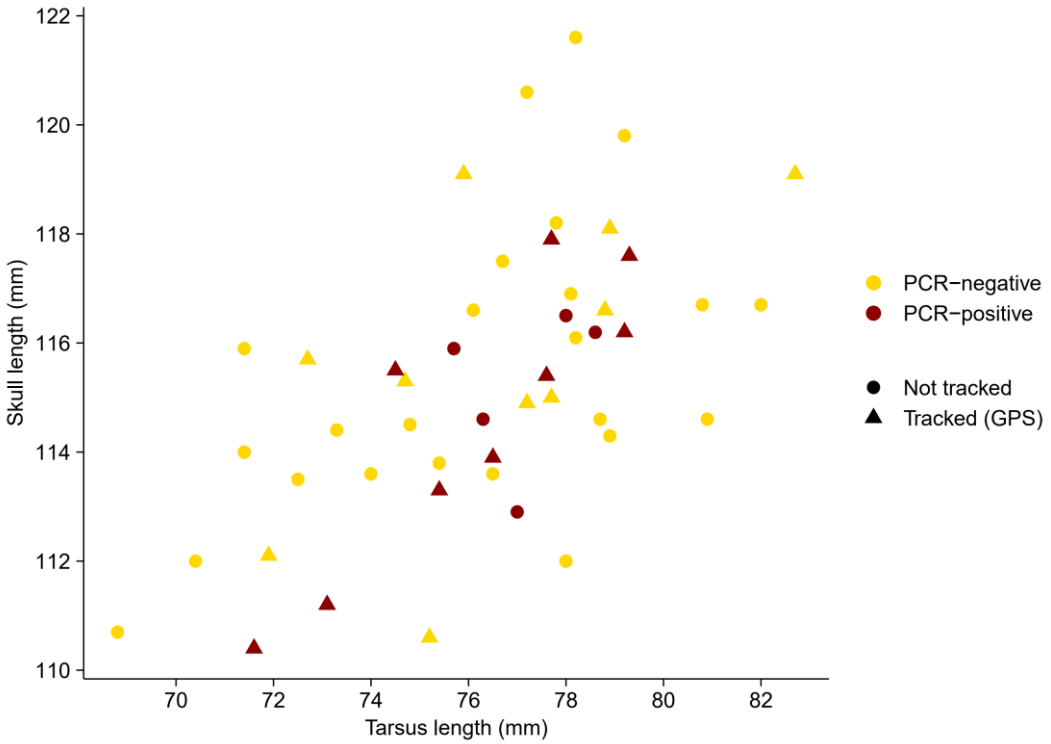

Figure S1.B.3. Size of sampled adult brown skuas. Colours of the dots indicates individual infections status according to the detection of *P. multocida* DNA in their cloacal swab, and shape indicates if the individual has been equipped with a GPS logger to track its movements. Data were collected from birds captured in 2015-2016 and 2016-2017 on Plateau des Tourbières and on Entrecasteaux and Mare aux Éléphants club, Amsterdam Island.

Size parameters (tarsus and skull lengths) of adult skuas showed a relatively important dispersion, suggesting that both males and females (females being usually larger than males; Furness, 1987) were included in the study. However, the distribution being not clearly bimodal, it was not possible to attribute a sex to the measured individuals with sufficient certainty to explore any potential effect of sex on birds' epidemiological status.

Appendix S1.C. Movement tracking: supplementary methods and results

Logger deployment

Solar-powered GPS-UHF devices (GPS-UHF Harrier-L®, Ecotone, Poland) were used. The loggers were programmed with a GPS acquisition frequency of 2 min in 2015-2016 and of 5 min in 2016-2017 in order to increase battery duration. A base station for data download was placed on the fringe of the plateau where skuas nest. The loggers were attached using a leg-loop harness in 2015-2016 (Thaxter *et al.* 2014). Rapid loss of several of the loggers and of battery power because of the bird wings covering the solar panels when not flying required an alternative attachment method. In 2016-2017, loggers were thus attached to the upper back feathers with Tesa® tape (Carneiro *et al.* 2014). All loggers shed off from equipped individuals within four months of deployment.

Table S1.C.1. Summary of tracking data collection on brown skuas. "Not at nest" locations refer to data after exclusion of locations recorded within the nesting area of the tracked individuals. Analyses were conducted on the 13 individuals for which data were collected for > 24h.

Year	Logger	Number of locations		Dates		Data collection duration (day)
		Total	Not at nest	First data	Last data	
2015-2016	HAR20	2748	644	03/12/2015	14/03/2016	102
	HAR21	902	81	03/12/2015	25/01/2016	53
	HAR23	3088	944	03/12/2015	11/01/2016	39
	HAR25	1075	167	03/12/2015	29/01/2016	64
	HAR29	88	9	06/12/2015	06/12/2015	0
2016-2017	HAR01	6122	1035	26/11/2016	01/02/2017	67
	HAR02	1177	432	26/11/2016	08/12/2016	12
	HAR03	1518	311	01/12/2016	24/02/2017	85
	HAR04	1285	216	01/12/2016	25/02/2017	86
	HAR06	91	133	02/12/2016	26/02/2017	86
	HAR07	571	39	02/12/2016	25/01/2017	54
	HAR08	728	62	02/12/2016	15/01/2017	44
	HAR09	1970	364	02/12/2016	18/01/2017	47
	HAR10	1713	316	02/12/2016	19/01/2017	48

Representativeness of the tracking sample

Following Lascelles *et al*. (2016), the representativeness of the sample (n = 14 tracked individuals with data out of the brown skua nesting area) was examined by randomly selecting individuals iteratively and comparing the randomly selected with the unselected data. For 200 random draws of sample sizes from 1 to 13 individuals, the contour of the 50% isopleth of the habitat use distribution ("core-use area") was computed from the sampled data. The inclusion value was then calculated as to the proportion of the unsampled data included within this core-use area. By fitting a nonlinear regression to the relationship between the inclusion value and the sample size, we could estimate the asymptote of this relationship. The sample size at which the data are assumed to fully represent the wider population is reached at the point where the rate of increase of the regression function decreases to zero (*i.e.,* when adding new samples simply replicates distributions already sampled). The maximum inclusion value achieved by the data was calculated

as the percentage of the estimated asymptote value, providing a measure of the representativeness of the sample. This metric thus represents how well the sampled data explain the habitat use of individuals in the unsampled data and if the tracking sample is therefore suitable for population-level inference.

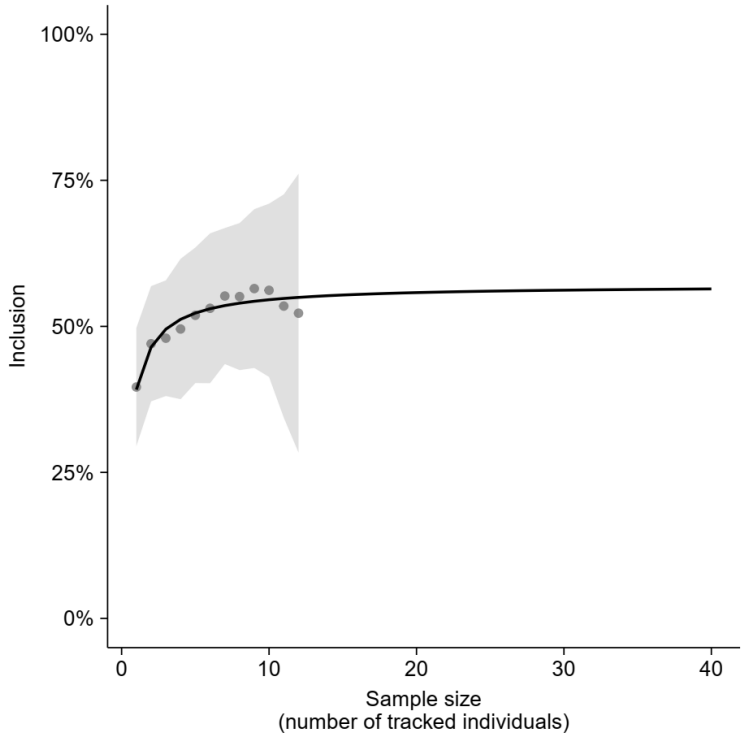

Figure S1.C.1. Assessing the representativeness of the tracking sample: the sample was estimated to represent 96% of the locations that would have been used by the entire sub-population of brown skuas breeding on southern PDT of Amsterdam Island during this period. The graph indicates what proportion of out-of-sample locations were located within the 50% core-use areas estimated from sampled locations (Inclusion value) for 200 random individual selections. The dots and the shaded area represent the mean ± standard deviation of the inclusion value, and the solid line represents the fitted nonlinear regression.

Individual data

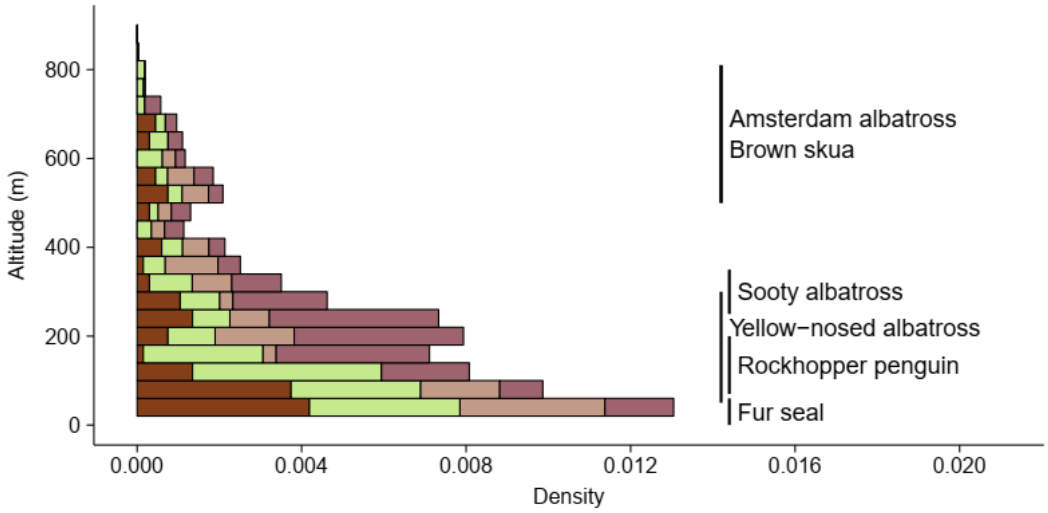

Figure S1.C.2. Altitudinal distribution of the locations of breeding brown skuas equipped with GPS-UHF loggers during the chick rearing period on Amsterdam Island in 2015-2016; each colour represents an individual and lines represent nesting altitudes of colonial species on Amsterdam Island.

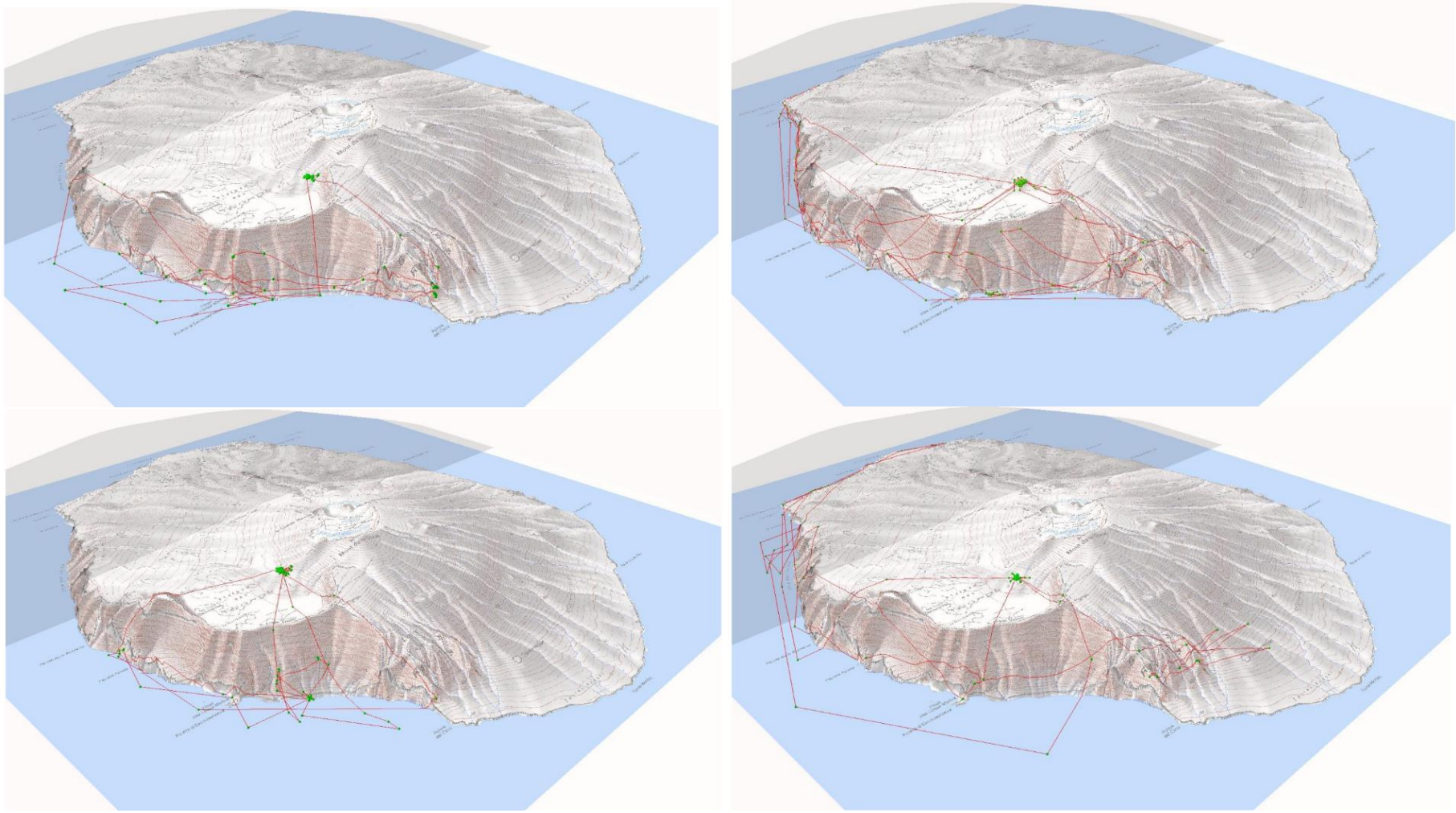

Figure S1.C.3. 3D representations of the movements of brown skuas over a 24h period (04/12/2015) of the chick rearing period on Amsterdam Island (37°49'S, 77°33'E) in 2015-2016. All locations are presented, including those recorded within the brown skua nesting area. Graphical representation courtesy of Yann Rantier, IPEV SUBANTECO-136/ECOBIO, Rennes.

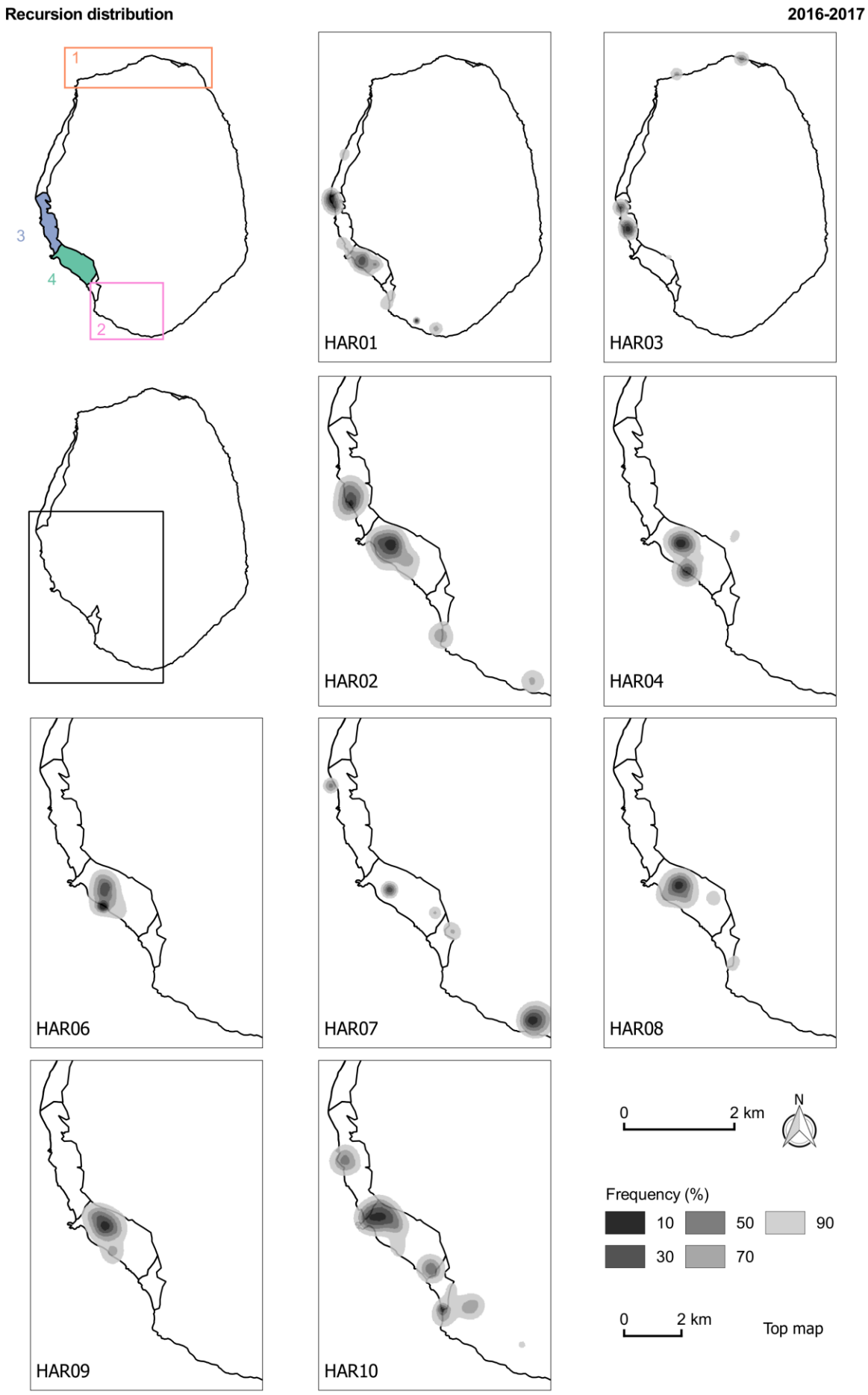
Recursion distribution
2016-2017
1
2
3
4
HAR01
HAR03
HAR02
HAR04
HAR06
HAR07
HAR08
HAR09
HAR10
0
2 km
N
Frequency (%)
10
50
90
30
70
0
2 km
Top map

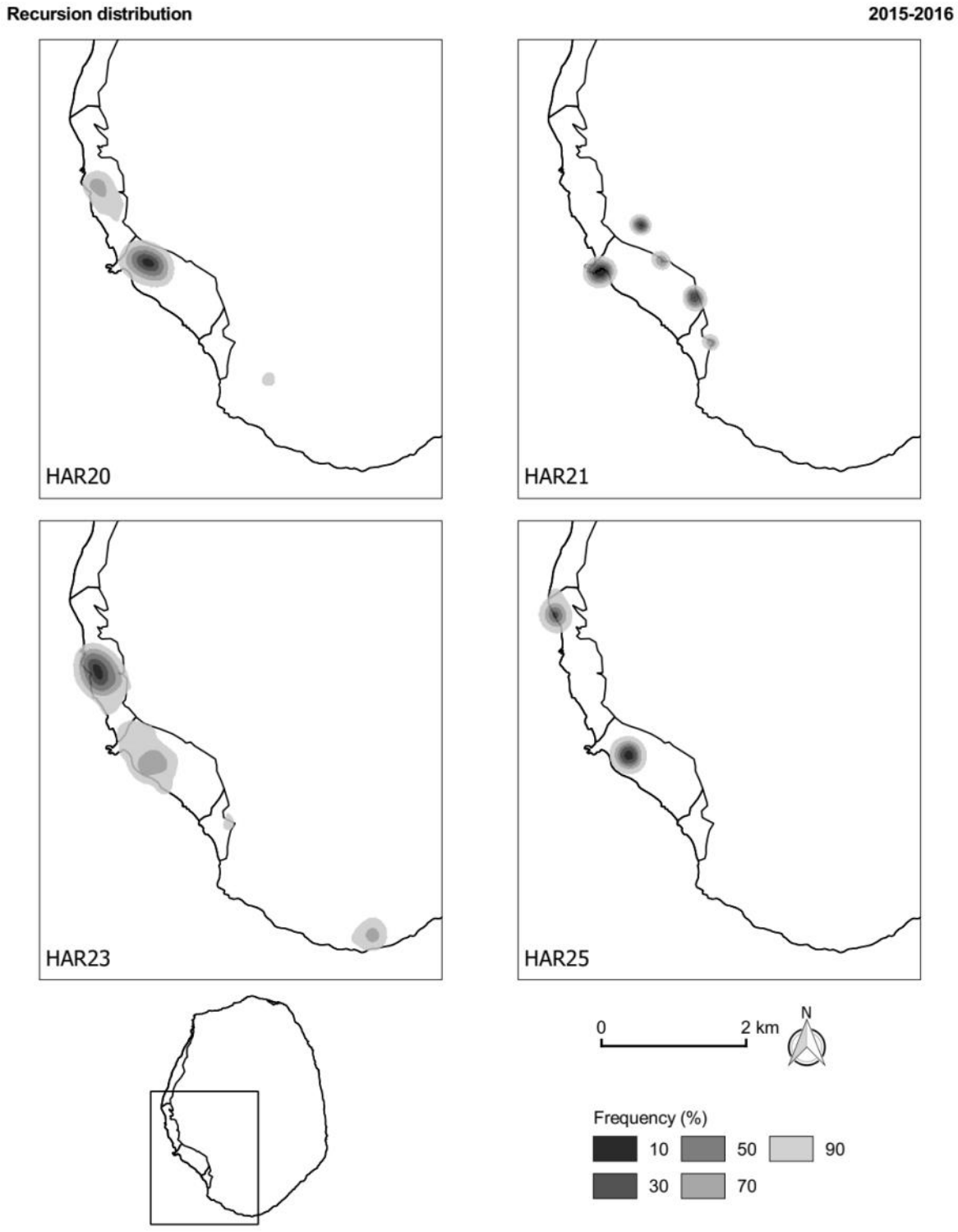

Figure S1.C.4. Recursion distribution of breeding brown skuas equipped with GPS-UHF loggers during the chick rearing period on Amsterdam Island (37°49'S, 77°33'E) in 2016-2017 (previous page) and in 2015-2016. These maps represent outputs of the BRB|MKDE program (Benhamou 2011; Benhamou & Riotte-Lambert 2012) delimiting non-overlapping virtual circles of 50 m in radius (hereafter referred to as "sites") and counting a new visit to this site each time the tracked individual re-entered it after a time lag spent outside the site longer than 10 min and remained in that site for at least 15 min. Inland recursion areas correspond to the surroundings of the skua nests. The top map represents the identified main foraging areas: (1) North coast, (2) South coast, (3) Northern part of the south-west cliff and (4) Southern part of the south-west cliff (corresponding to Entrecasteaux).

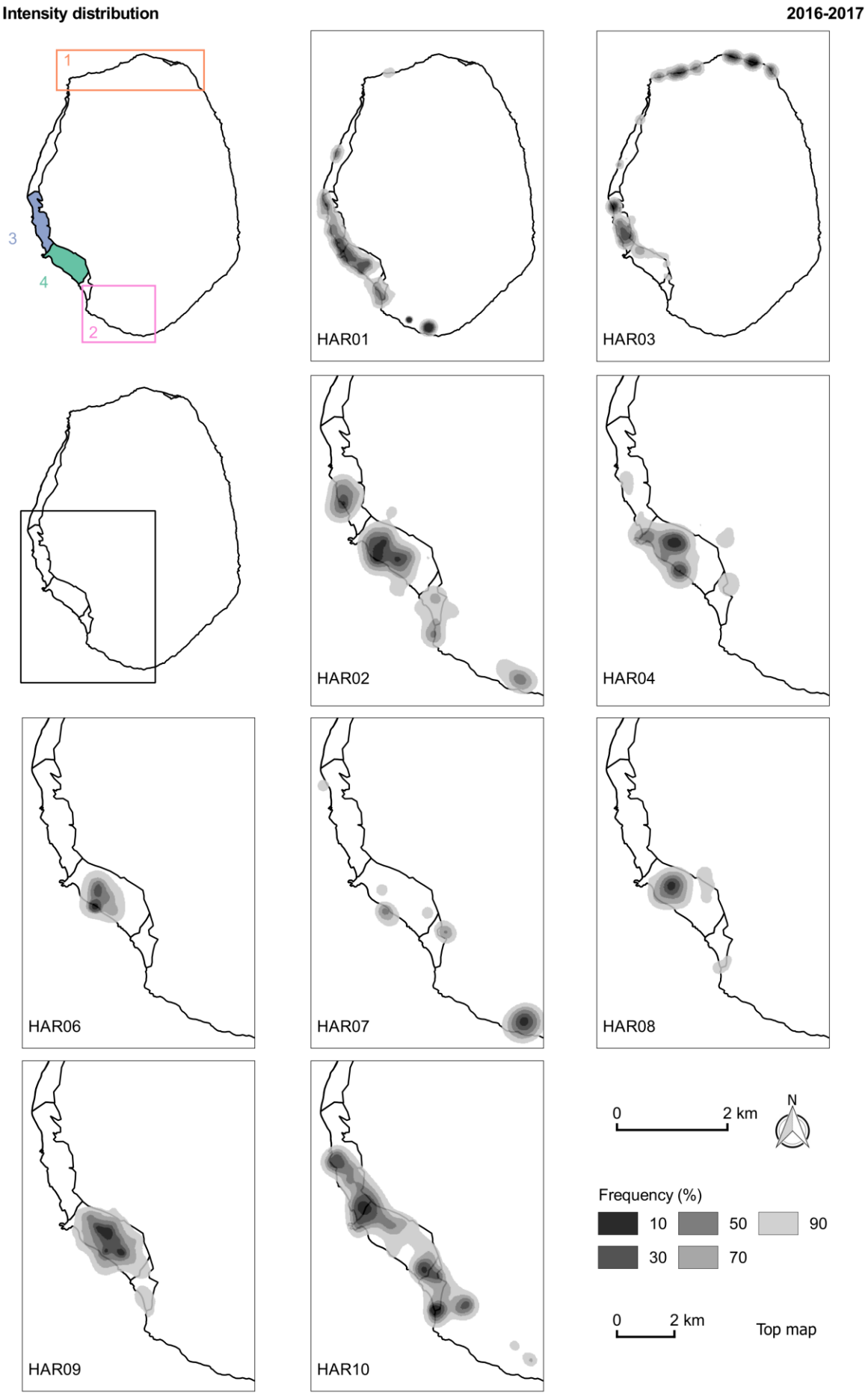
Intensity distribution
2016-2017
1
2
3
4
HAR01
HAR03
HAR02
HAR04
HAR06
HAR07
HAR08
HAR09
HAR10
0
2 km
N
Frequency (%)
10
50
90
30
70
0
2 km
Top map

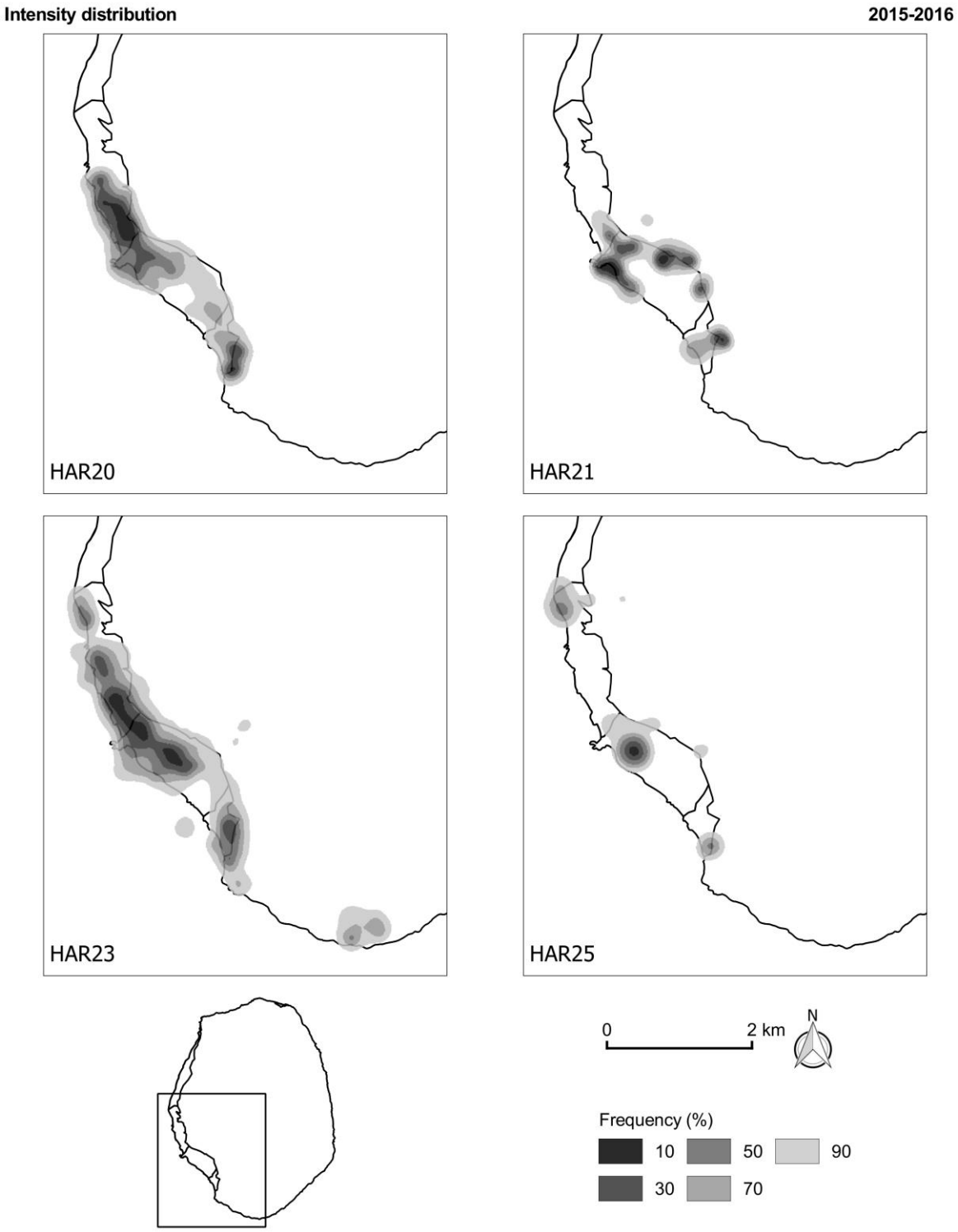

Figure S1.C.5. Intensity distribution of breeding brown skuas equipped with GPS-UHF loggers during the chick rearing period on Amsterdam Island (37°49'S, 77°33'E) in 2016-2017 (previous page) and in 2015-2016. These maps represent outputs of the BRB|MKDE program (Benhamou 2011; Benhamou & Riotte-Lambert 2012) delimiting non-overlapping virtual circles of 50 m in radius (hereafter referred to as "sites") and counting a new visit to this site each time the tracked individual re-entered it after a time lag spent outside the site longer than 10 min and remained in that site for at least 15 min. Inland recursion areas correspond to the surroundings of the skua nests. The top map represents the identified main foraging areas: (1) North coast, (2) South coast, (3) Northern part of the south-west cliff and (4) Southern part of the south-west cliff (corresponding to Entrecasteaux).

Table S1.C.2. Summary of sites recursively used by individual brown skuas and of their epidemiological status at the time of equipment. Recursive use information are based on GPS locations and recursion distributions represented on Figure S1.C.4. The four delimited zones are defined on Figure S1.C.3. Individuals equipped with the loggers HAR21, HAR06, HAR08 and HAR09 recursively used only the site of Entrecasteaux (southern part of the large costal cliff). All other individuals also recursively used other sites. ✓: site repeatedly visited by the individual; +: sero- or PCR-positive; -: sero- or PCR-negative.

		Recursive use				Epidemiological status	
Year	**Logger**	**North coast**	**South plain**	**Northern part of the south-west cliff**	**Southern part of the south-west cliff (Entrecasteaux)**	**Seropositive**	**PCR-positive**
2015-2016	HAR20		✓	✓	✓	+	+
	HAR21				✓	+	-
	HAR23		✓	✓	✓	+	-
	HAR25			✓	✓	+	-
2016-2017	HAR01		✓	✓	✓	+	+
	HAR02		✓	✓	✓	+	+
	HAR03	✓		✓	✓	+	+
	HAR04			✓	✓	+	+
	HAR06				✓	+	+
	HAR07			✓	✓	+	-
	HAR08				✓	+	+
	HAR09				✓	+	+
	HAR10		✓	✓	✓	+	-

Given species distribution on Amsterdam island (Figure 1 in the main text), we expect time spent by brown skuas in the south-west cliff to correspond to foraging in seabird and fur seal colonies and time spent on the north coast to foraging in fur seal colonies. In contrast, the density of seabirds and fur seal on the south plain is lower (no suitable habitat for cliff nesting seabirds, and low frequentation by fur seals; Guinet et al., 1994) and skuas probably mostly prey on introduced rodents (personal observations). Note that rodents are also observed in seabird and fur seal colonies, hence skuas foraging there may also feed on rodents (Figure S1.A.2).

Appendix S1.D. Timing and extent of epizootics in yellow-nosed albatross nestlings in relation to skua activities

In order to determine the timing and extent of epizootics affecting yellow-nosed albatrosses in relation to skua activities, monitoring was conducted during the breeding seasons 2015-2016 and 2016-2017. A naturally delimited subcolony of approximately 250 breeding pairs of yellow-nosed albatrosses in Entrecasteaux was surveyed as part of a vaccination experiment of albatross nestlings against *P. multocida* (Bourret *et al.* 2018). This vaccine having proven its efficiency to improve nestling survival during avian cholera epizootics (Bourret *et al.* 2018), only non-vaccinated nestlings were included in the calculation of the proportion of surviving nestlings. Each year, about 30 nests were tagged during the hatching period in December and the presence of the nestling was recorded once a month until fledging in late March.

Current infection by *P. multocida* was also assessed in these yellow-nosed albatross nestlings by RT-PCR conducted on cloacal swabs. In order to increase the sample size, and because the mortality rate was high in non-vaccinated nestlings, the calculation of prevalence also included nestlings vaccinated against *P. multocida*. Nestlings were captured by hands and handled on their nest. The design used for molecular detection of *P. multocida* DNA from cloacal swabs of yellow-nosed albatross nestlings was similar to the one used with brown skua samples.

Table S1.D.1. Proportions of yellow-nosed albatross nestlings from Amsterdam Island positive for *P. multocida* DNA based on RT-PCR from cloacal swabs. Clopper-Pearson 95% confidence intervals are indicated between brackets and numbers of occupied/observed nests or positive/tested individuals between parentheses.

Month	Nestling survival	Proportion of *P. multocida* positive nestlings
December 2015	1.00 [0.90;1.00] (35/35)	0.09 [0.03;0.21] (5/53)
January 2016	0.77 [0.60;0.90] (27/35)	0.66 [0.5;0.8] (29/44)
February 2016	0.35 [0.20;0.54] (12/34)	1.00 [0.85;1.00] (22/22)
March 2016	0.12 [0.03;0.27] (4/34)	0.87 [0.60;0.98] (13/15)
December 2016	1.00 [0.89;1.00] (31/31)	0.00 [0.00;0.07] (0/48)
January 2017	0.61 [0.42;0.78] (19/31)	0.47 [0.29;0.65] (15/32)
February 2017	0.13 [0.04;0.30] (4/31)	0.67 [0.22;0.96] (4/6)
March 2017	0.06 [0.01;0.21] (2/31)	0.70 [0.35;0.93] (7/10)

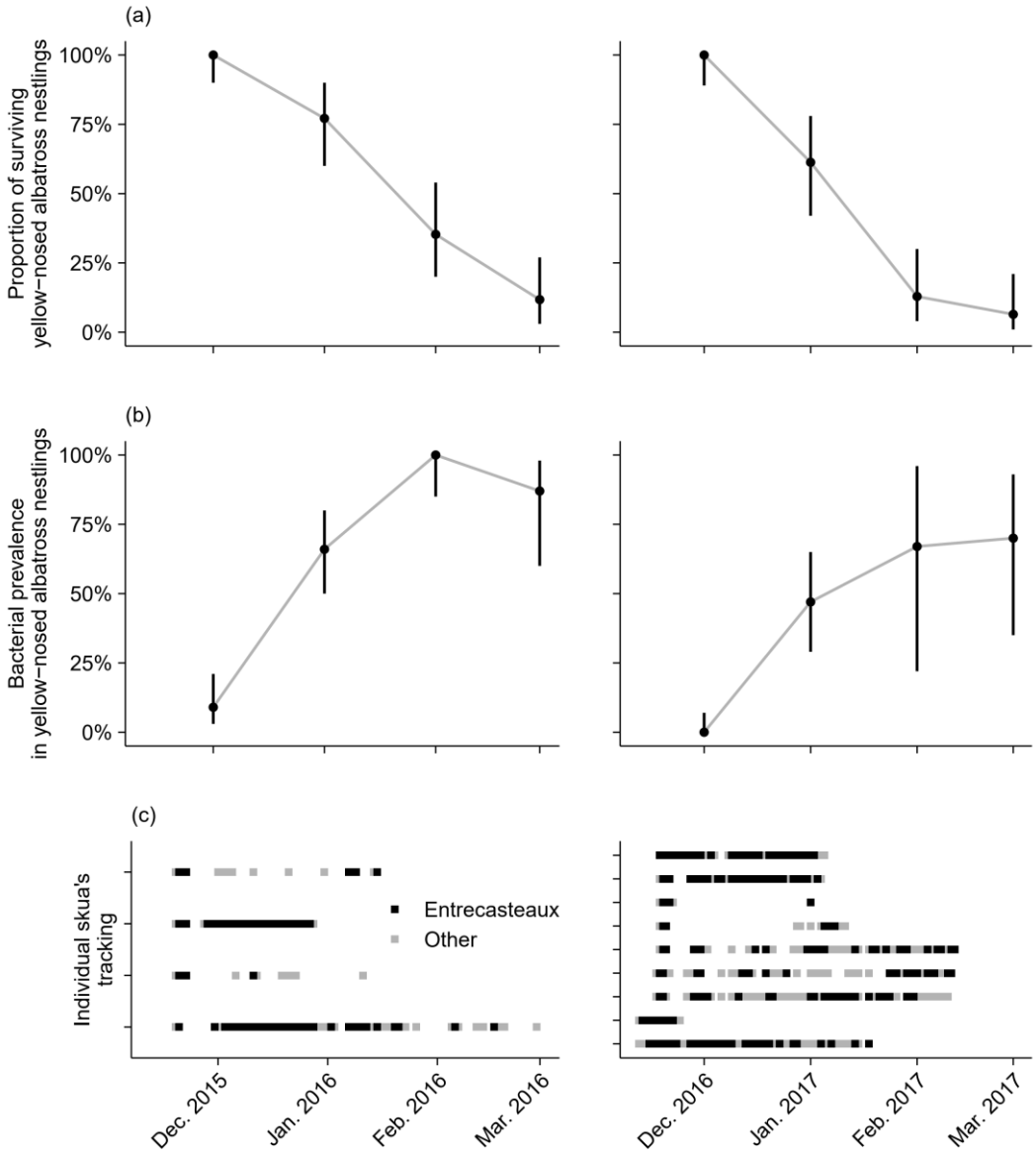

Figure S1.D.1. Avian cholera epizootic dynamics in a yellow-nosed albatross colony on Amsterdam Island during the 2015-2016 and 2016-2017 breeding seasons and timing of movement tracking of breeding brown skuas. Proportion of yellow-nosed albatross nestlings surviving **(a)** and positive for *P. multocida* DNA **(b)** in the monitored subcolony of Entrecasteaux between hatching and fledging; bars represent the 95% Clopper Pearson confidence interval and sample sizes are given in Table S1.D.1. Recorded locations of breeding brown skuas **(c)** outside of Entrecasteaux (grey) or in Entrecasteaux (black); blank periods between locations correspond to low battery periods preventing data recording.

Appendix S1.E. Brown skua nestling infection status and serology

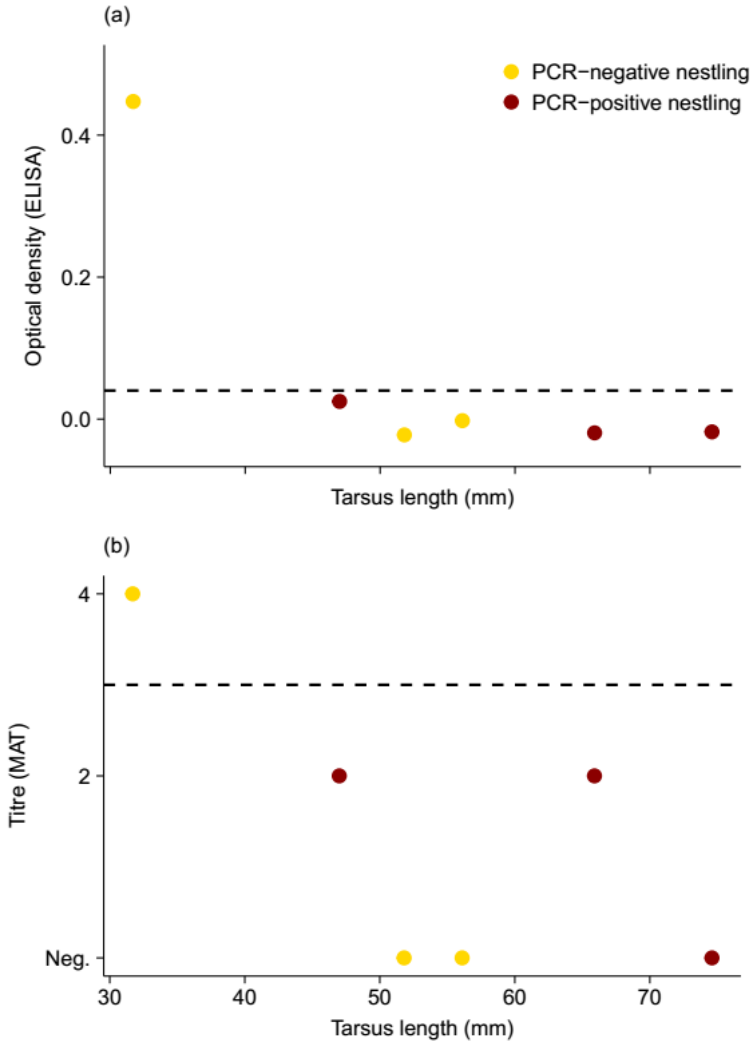

Figure S1.E.1. *P. multocida* specific antibody levels in brown skua nestlings measured by ELISA **(a)** or MAT **(b)** in relation to their tarsus length as a proxy of age. Samples were collected in December 2016 on Plateau des Tourbières, Amsterdam Island. The seropositivity threshold values are represented by dashed lines. Colour of the dots indicates individual current infection status according to the detection of *P. multocida* DNA in their cloacal swab. Antibodies detected in the younger nestling (shorter tarsus) could be maternally inherited considering its PCR-negative status and the high seroprevalences observed in breeding adults. PCR-positive nestlings in which antibodies have not been detected may likely correspond to recently exposed individuals that have not mounted an immune response yet at the time of sampling.

Considering that *P. multocida* appears to mostly impact nestlings in albatrosses (Gamble et al., 2019), its potential impact on skua nestlings remains to be quantified. As observed in other seabird-parasite systems (Gasparini et al., 2002; Garnier et al., 2012) and considering the high seroprevalence in adults, antibodies detected in nestlings are likely maternal antibodies transferred from the breeding females to their offspring via the egg yolk. If these antibodies could confer a temporary passive protection of young offspring against pathogens, it would open perspectives for the protection of albatross nestlings through the vaccination of their mothers (Bourret et al., 2018; Gamble et al., 2019).

Appendix S1.F. Schematization of the epidemiological network

The schematized epidemiological network (Figure 2b) was drawn based on relative time spent in different areas of interest corresponding to albatross and penguin nesting areas. Edge widths between skuas and other species represent the relative time spent in each potential foraging area approximated by the proportion of locations recorded in a given delimited space among all locations recorded outside of the skua nesting area. Edge widths between two skuas represent the probability of two skuas being present in the same potential foraging area at the same time noted $P(encounterSkua_iSkua_j)$ and calculated as:

$$P(encounterSkua_iSkua_j) = \bigcup_{n=1}^{N}(Skua_i \in Area_n) \cap (Skua_j \in Area_n)$$

corresponding to

$$P(encounterSkua_iSkua_j) = \sum_{n=1}^{N} P(Skua_i \in Area_n) \times P(Skua_j \in Area_n)$$

with $P(Skua_i \in Area_n)$ being approximated by the relative time spent by the individual $Skua_i$ in the $Area_n$ and N the number of considered areas and under the assumptions that $Skua_i \in Area_n$ and $Skua_j \in Area_n$ are independent events. This assumption seems reasonable considering the observed absence of feeding territory defence behaviours during the tracking period.

The resulting schematized epidemiological network was drawn using the '*igraph*' R package (Csardi & Nepusz 2006).

References

Benhamou, S. (2011). Dynamic approach to space and habitat use based on biased random bridges. *PLOS ONE*, 6, e14592.

Benhamou, S. & Riotte-Lambert, L. (2012). Beyond the utilization distribution: identifying home range areas that are intensively exploited or repeatedly visited. *Ecological Modelling*, 227, 112–116.

Bourret, V., Gamble, A., Tornos, J., Jaeger, A., Delord, K., Barbraud, C., Tortosa, P., Kada, S., Thiebot, J.-B., Thibault, E., Gantelet, H., Weimerskirch, H., Garnier, R. & Boulinier, T. (2018). Vaccination protects endangered albatross chicks against avian cholera. *Conservation Letters*, e12443.

Carneiro, A.P.B., Manica, A. & Phillips, R.A. (2014). Foraging behaviour and habitat use by brown skuas *Stercorarius lonnbergi* breeding at South Georgia. *Marine Biology*, 161, 1755–1764.

Csardi, G. & Nepusz, T. (2006). The igraph software package for complex network research. *InterJournal, Complex Systems*, 1695, 1–9.

Fleiss, J.L. (1981). *Statistical Methods for Rates and Proportions.* 2nd edn. Wiley, John and Sons, Incorporated, New York.

Furness, R.W. (1987). *The Skuas*. A&C Black, London.

Gamble, A., Garnier, R., Jaeger, A., Gantelet, H., Thibault, E., Tortosa, P., Bourret, V., Thiebot, J.-B., Delord, K., Weimerskirch, H., Tornos, J., Barbraud, C. & Boulinier, T. (2019). Exposure of breeding albatrosses to the agent of avian cholera: dynamics of antibody levels and ecological implications. *Oecologia* 189, 939–949.

Garnier, R., Graham, A.L. (2014). Insights from parasite-specific serological tools in eco-immunology. *Integrative and Comparative Biology* 54, 363–376.

Garnier, R., Ramos, R., Sanz-Aguilar, A., Poisbleau, M., Weimerskirch, H., Burthe, S., Tornos, J. & Boulinier, T. (2017). Interpreting ELISA analyses from wild animal samples: some recurrent issues and solutions. *Functional Ecology*, 31, 2255–2262.

Garnier, R., Ramos, R., Staszewski, V., Militão, T., Lobato, E., González-Solís, J., & Boulinier, T. (2012). Maternal antibody persistence: a neglected life-history trait with implications from albatross conservation to comparative immunology. *Proceedings of the Royal Society of London B: Biological Sciences*, 279, 2033–2041.

Gasparini, J., McCoy, K. D., Tveraa, T., & Boulinier, T. (2002). Related concentrations of specific immunoglobulins against the Lyme disease agent Borrelia burgdorferi sensu lato in eggs, young and adults of the kittiwake (*Rissa tridactyla*). *Ecology Letters*, 5, 519–524.

Guinet, C., Jouventin, P., & Georges, J.-Y. (1994). Long term population changes of fur seals *Arctocephalus gazela* and *Arctocephalus tropicalis* on subantarctic (Crozet) and subtropical (St. Paul and Amsterdam) islands and their possible relationship to El Nifio Southern Oscillation. *Antarctic Science*, 6, 473–478.

Heerah, K., Dias, M. P., Delord, K., Oppel, S., Barbraud, C., Weimerskirch, H., & Bost, C. A. (2019). Important areas and conservation sites for a community of globally threatened marine predators of the Southern Indian Ocean. *Biological Conservation*, 234, 192–201.

Jaeger, A., Gamble, A., Lagadec, E., Lebarbenchon, C., Bourret, V., Tornos, J., Barbraud, C., Lemberger, K., Delord, K., Weimerskirch, H., Thiebot, J.-B., Boulinier, T., Tortosa, P. (2019). Exploring the infection

dynamics of a bacterial pathogen on a remote oceanic island reveals annual epizootics impacting an albatross population. *BioRxiv*, 711283.

Jaeger, A., Lebarbenchon, C., Bourret, V., Bastien, M., Lagadec, E., Thiebot, J.-B., Boulinier, T., Delord, K., Barbraud, C., Marteau, C., Dellagi, K., Tortosa, P. & Weimerskirch, H. (2018). Avian cholera outbreaks threaten seabird species on Amsterdam Island. *PLOS ONE*, 13, e0197291.

Lascelles, B.G., Taylor, P.R., Miller, M.G.R., Dias, M.P., Oppel, S., Torres, L., Hedd, A., Le Corre, M., Phillips, R.A., Shaffer, S.A., Weimerskirch, H., Small, C. & Visconti, P. (2016). Applying global criteria to tracking data to define important areas for marine conservation. *Diversity and Distributions*, 22, 422–431.

Legendre, P. (2013). *Model II Regression*.

Lobato, E., Pearce-Duvet, J., Staszewski, V., Gómez-Díaz, E., González-Solís, J., Kitaysky, A., McCoy, K.D. & Boulinier, T. (2011). Seabirds and the circulation of Lyme borreliosis bacteria in the North Pacific. *Vector-Borne and Zoonotic Diseases*, 11, 1521–1527.

Longmire, J.L., Lewis, A.K., Brown, N.C., Buckingham, J.M., Clark, L.M., Jones, M.D., Meincke, L.J., Meyne, J., Ratliff, R.L. & Ray, F.A. (1988). Isolation and molecular characterization of a highly polymorphic centromeric tandem repeat in the family Falconidae. *Genomics*, 2, 14–24.

Revelle, W. (2014). psych: procedures for psychological, psychometric, and personality research. *Northwestern University, Evanston, Illinois*, 165.

Thaxter, C.B., Ross-Smith, V.H., Clark, J.A., Clark, N.A., Conway, G.J., Marsh, M., Leat, E.H.K. & Burton, N.H.K. (2014). A trial of three harness attachment methods and their suitability for long-term use on lesser black-backed gulls and great skuas. *Ringing & Migration*, 29, 65–76.

Tizard, I. R. (2004). *Veterinary Immunology: an introduction.* 7th edn. Saunders.